J Sol-Gel Sci Techn (2007) 41:277–289
DOI 10.1007/s10971-006-9006-2

Preparation and optical characterization of catalyst free SiO_2 sonogel hybrid materials

Omar G. Morales-Saavedra · Ernesto Rivera · José O. Flores-Flores · Rosalba Castañeda · José G. Bañuelos · José M. Saniger

Received: 23 June 2006 / Accepted: 8 September 2006 / Published online: 20 December 2006

Abstract The synthesis of sol-gel materials induced by ultrasonic irradiation (sonolysis) is implemented as an alternative method for the fabrication of highly pure organic-inorganic composites with good monolithic, mechanical and optical properties. Ultrasonic irradiation, instead of commonly used basic- or acidic-catalyst was used to produce acoustical cavitation within the liquid H_2O/tetraethylortosilicate (TEOS) reactants. This procedure forms a hydrolyzed-TEOS colloidal dispersion (sol) which produces, after drying, a highly pure SiO_2 network. The resulting SiO_2 glass exhibits high porosity and allows the inclusion of several organic compounds in the colloidal sol-state. Novel, optical active synthesized liquid crystalline (LC)-azo-compounds, bent shaped mesogens, *cis*- and *trans*-poly(1-ethynylpyrene)s, as well as fullerene (C_{60}) spheres and classical organic dyes were successfully incorporated as dopant agents within the novel catalyst free (CF) SiO_2-sonogel host matrix. Absorption and fluorescence spectroscopy studies were carried out in order to characterize the optical performance of both the CF-sonogel and several hybrid composites The pulsed laser photoacoustic technique (LPAT) was implemented to determine thermodynamic phase transitions of LC-based hybrids and laser induced damage (photodegradation) in dye-based composites. Finally, comparative morphology studies between undoped reference samples and some doped composites were performed by Atomic Force Microscopy (AFM), where an optimal TEOS/dopant concentration ratio, to obtain good mechanical properties among the studied samples, has been found.

Keywords Sonolysis · Sol-gel · Sonogels · Photoacoustic · Hybrid materials · NLO-materials

O. G. Morales-Saavedra (✉) · J. O. Flores-Flores · R. Castañeda · J. G. Bañuelos · J. M. Saniger
Centro de Ciencias Aplicadas y Desarrollo Tecnológico, CCADET-UNAM, Circuito Exterior, Ciudad Universitaria, Apartado Postal 70-186 Coyoacán, México D.F., C.P. 04510, México
e-mail: omar.morales@ccadet.unam.mx, omardel@gmail.com

E. Rivera
Instituto de Investigaciones en Materiales, IIM-UNAM, Circuito Exterior, Ciudad Universitaria, Coyoacán, México D.F., C.P. 04510, México

1 Introduction

The sol-gel technique has been intensively used over the past twenty years as a standard method to confine and encapsulate diverse dopant species into a glassy SiO_2 matrix in order to prepare advanced materials with interesting physical properties [1–6]. Potential applications have been proposed in recent years for organic doped SiO_2 networks in several research fields like nonlinear photonics, photochromic materials, photorefractivity, sensing devices, biomedicine and tunable solid state dye laser systems, among others [7–14]. The investigation of nonlinear optical (NLO)-processes are of particular interest since they offer potential applications in photonics. Emphasis has been put on materials suitable for electro-optical systems and integrated optical circuits adopting the guided-wave format, which provides additional alternatives to the conception and production of photonic and telecommunication devices. Beside materials such as push-pull polymers, recently ferroelectric liquid crystals have been also intensively investigated regarding their NLO properties, for instance second harmonic generation (SHG) and optical limiting [6, 15–19]. It has been a difficult task, however, to combine the synthesis of many of these promising polar molecules with the desired optical properties, usually expected in the solid-state and at room temperature [6, 19, 20].

The optimal inclusion of these molecules into an amorphous inorganic SiO_2 matrix to provide alternative low cost optical materials has been also a challenging task of current interest [8, 15]. Other important aspects to be considered in the development of efficient devices suitable for optical sciences and photonics is the material malleability and the mechanical stability, which are necessary in several technological implementations, for instance in waveguiding and quasi-phase-matched (QPM) structures [19, 21, 22]. For these applications, deposition of organic spin-coated thin films is required to fill up several optical channels and circuitry, which have to remain stable for long periods of time. Polymerization of liquid crystalline mesogens as well as the combination of organic optical chromophores within guest-host polymeric systems have been recently reported in order to generate more stable and solid structures once they have been dissolved and spin-coated into the waveguiding channels produced by standard photolithographic techniques [19].

From the sol-gel sciences point of view, easy material processing offered by the colloidal state and recent developments on the deposition of doped sol-gel thin film layers, satisfy largely the requirements mentioned above [6]. Since the SiO_2 gelation process takes long time before the doped colloidal mixture reaches a dry and stable state, it allows an efficient deposition of doped colloidal dispersions (sols) onto the micrometric integrated structures registered in different kinds of wafers and substrates. The high malleability of these materials permits them to adopt a very wide variety of shapes required for photonic proposes. *In situ* poling of the dopant-species is also possible, in order to improve their NLO-performance. Once the drying process is completed, the rigidity of the hybrid sol-gel material in the desired format can be achieved. The constituting organic compounds will contribute to a desired physical or chemical property, whereas the inorganic part of the hybrid composite increases its mechanical and thermal strength [23, 24]. These materials can show, depending on the purity of the sol-gel precursor solvents, a very stable behavior within a wide range of temperatures. Thus, the different optical properties of the dopant species are preserved, without decomposition of the fragile guest molecules.

In this work, we report the development of several hybrid materials, implementing novel and promising molecular systems, which may have huge potential for different optical and photonic applications. For this purpose, we exploited the novel catalyst-free sonolysis route to produce highly pure sol-gel samples generated by ultrasonic irradiation (sonogel materials). This new approach has been very recently developed in our group [25]. The sol-gel materials obtained by this method exhibit an amorphous SiO_2-matrix with large surface areas, high purity level and nanometric porosity, which represent a favorable environment for the inclusion of interesting organic chromophores. In order to generate CF-sonogel materials, energetic pulsed ultrasonic waves, instead of the use of acidic and basic catalyst, are applied at the TEOS/H_2O reactants interface to produce acoustical cavitation. This procedure starts the sono-chemical reaction necessary to prepare a highly pure SiO_2 solid networks [25]. We demonstrate in this work, that the novel CF-sonogel materials can be easily doped in the colloidal state with several interesting optically active compounds, which are currently being considered as promising materials for different technological applications. Azobenzene compounds, bent-shaped liquid crystalline mesogens, fullerene (C_{60}) spheres, conjugated *cis*- and *trans*-poly(pyrenylacetylene)s and classical organic dyes such as Rhodamine 590, Nile-Blue 690, Stilbene 420 and Coumarin 440, were successfully incorporated in solution as dopant agents in the bulk material of CF-sonogels. Some of these compounds have been specially designed for optical photo-alignment and second order NLO-effects. The synthesis and some optical properties (in solution) of these molecular structures have been recently reported in the literature [26–31]. After drying, the formed hybrid composites showed good physical properties suitable for several optical applications: high dopant concentrations, high microstructural homogeneity, stable mechanical properties (geometric monolith structure), high optical quality and high laser damage thresholds.

The experimental results shown in this paper have been carried out as a primary and explorative work in the development of photonic organic-inorganic prototypes, where the implementation of the novel and highly pure CF-sonogels plays an important role. This may provide practical alternatives to expensive inorganic crystals, where the use of low cost and specifically designed optical chromophores, is desirable.

2 Experimental section

2.1 Catalyst free SiO_2 sonogel sample preparation

The sol-gel method frequently used to synthesize amorphous SiO_2, based on the hydrolysis of different precursors such as TEOS, TMOS, etc., followed by condensation reactions of the hydrolyzed species, has been widely adopted as a suitable way to obtain glassy doped materials with good optical quality. Both, hydrolysis and condensation reactions occur normally in the presence of acidic or basic catalysts, where ethanol or methanol are commonly used as standard solvents for the precursor and water reactants. Fundamental and experimental details for the sol-gel synthesis of SiO_2 can be found extensively in the literature [1]. On the other hand, several articles reporting emulsification action of the reactive mixtures induced by ultrasonic irradiation have been published in recent years, where no solvents are used

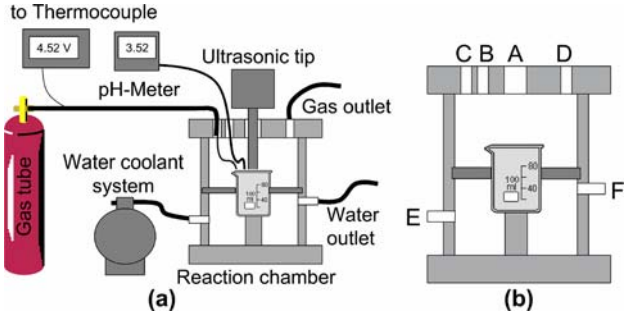

Fig. 1 (a) Experimental device for catalyst free sonogel sample preparation and (b) Details of the reaction chamber: (A) Ultrasonic tip, (B) pH-electrode, (C) Gas inlet, (D) Gas outlet, (E) Cooling water inlet, (F) Cooling water outlet

[32–35]. In such way, it is possible to obtain sonolyzed-gel materials with an elastic modulus several orders of magnitude higher than those prepared by conventional methods [36]. In this contribution, a new approach for the preparation of highly pure SiO_2 sonogels is exploited. Here, the use of both, solvents and catalysts is evaded at all. The hydrolyzed species are substituted by molecular radicals generated by ultrasound (extensive details on the synthesis, chemistry and methodology to produce this new kind of materials, can be found in reference [25]). In the present article, only a brief explanation of this new approach is presented in order to clarify the procedure to obtain CF-sonogel SiO_2 matrices as host materials for organic compounds and the development of CF-hybrid composites.

Figure 1 shows the experimental device used to produce sonogel samples. A two compartments polymetacrylate cylinder was implemented as reaction chamber. A hole in the middle point of the chamber lid acts as support for a Pyrex glass vessel (100 mL), which is the reaction container. Two neoprene o-rings seal the upper from the lower part of the chamber allowing perfect isolation conditions. Several holes placed on the top and the wall of the reaction chamber permit different applications:

Hole (A) serves as an input for the ultrasonic tip (with 1.25 cm diameter); hole (B) is used to introduce electrodes in order to sense the pH-value continuously. Holes (C) and (D) are used as input and output valves in order to regulate a selected gas-flow, which rules the reaction environment of the system. Moreover, a thermocouple (type K) is also introduced trough hole (C), parallel to the feed pipe of the selected gas, so that the reaction temperature can be accurately sensed. For the present application, only an oxygen-environment was employed (300 mL min^{-1}), because it has been shown that this atmosphere provides optimal conditions for the fabrication of hybrid SiO_2 networks with the current methodology. Points E and F correspond to the input and output valves of a water cooling system, which controls the reaction temperature. Low temperature conditions (∼5°C) should be maintained in order to avoid excessive overheating of the reactant water produced by energetic ultrasonic wave irradiation.

As precursor solution, 25 mL of tetraethyl-ortosilicate (TEOS, Fluka 99% purity) and 25 mL of three-distilled water were mixed into the glass vessel. The three-distilled water was previously boiled in order to eliminate dissolved gases and then cooled to room temperature. The initial pH-value of water was 6.5. In order to avoid any possible over-heating of the reactants by the incidence of ultrasonic waves, the temperature was stabilized at 1°C for 1 h before irradiation. The tip of the ultrasonic-wave generator (Cole-Parmer-CPX) acts also as an ultrasonic-homogenizer. The experimental system was sealed and isolated from room conditions, while an oxygen tube (AGA-ONU1072) was coupled to hole (C) to fix the reaction atmosphere. Before ultrasonic irradiation, the selected gas was bubbled for ca. 15 min through the vessel. The metallic ultrasound tip, carefully located at the TEOS/H_2O surface interface, was then started at 60 Hz and 180 W (effective irradiation power density was in the order of 3.2 W/cm^3). Oxygen flow was maintained during the whole sonolysis process. After 3 h of programmed ultrasonic irradiation (on/off-intermittent sequences of 5 s. net irradiation time: 1.5 h), the sonicated suspension was kept in the reactor. Twenty four hours after irradiation, two immiscible phases appear: the upper corresponding to unreacted TEOS, whereas the lower phase is a stable colloidal suspension containing the sonication induced hydrolyzed product (OH-TEOS). The unreacted TEOS was then removed, while the remaining colloidal suspension (OH-TEOS or sonicated product) was dropped and metered at different volumes into cylindrical teflon-containers. Several dopant molecules, previously dissolved in THF were afterwards added to the deposited colloidal suspension in order to start the gelation process and the inclusion of dopants within the CF-SiO_2 matrix. Rigid monolithic samples, adequate for optical characterization were obtained after two weeks of aging. The resulting bulk hybrids possess higher purity compared to other traditional synthesized sol-gel hybrid composites, because the use of the ultrasonic waves instead of reactive solvents and catalyst, gives samples with higher optical quality. In order to investigate the purity of the obtained CF-sonogels, comparative absorption and photoluminescence (PL) studies were carried out between our sonicated CF-product and some sonogels prepared by the same route with additional nitric acid as catalyst. As expected, the incorporation of only 0.1 mL of HNO_3 (65.5%, from J. T. Baker, molar concentration: 14.72 M) to the 25–25 mL of TEOS-H_2O, induced a faster sono-chemical reaction and consequently a faster gelation process. After only 3 min of intermittent ultrasonic irradiation, a homogeneous phase was obtained, where 100% of the TEOS precursor was hydrolyzed. After 24 h of aging only (atmosphere conditions: $T = 40$°C),

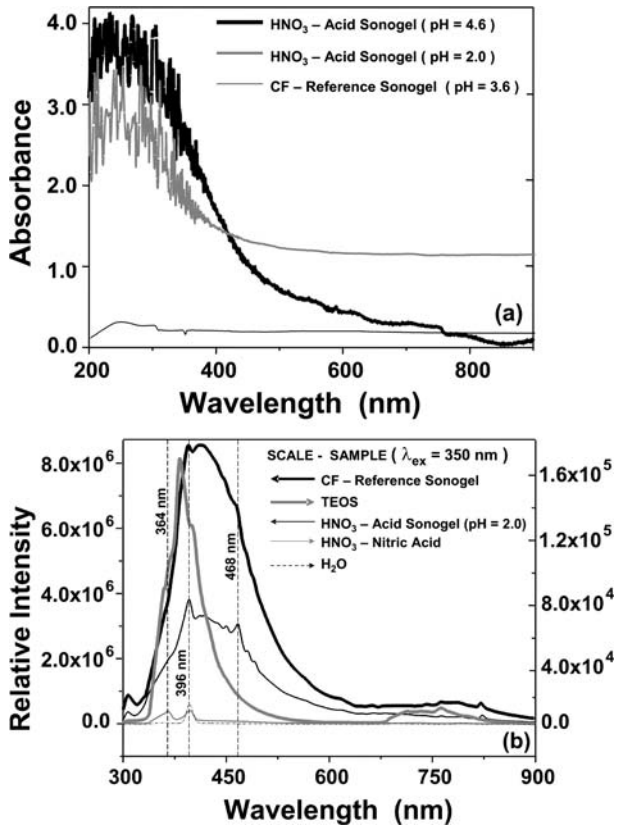

Fig. 2 (a) Comparative absorption spectra of a reference CF-sonogel and different HNO_3 catalyzed sonogels. (b) Comparative PL-spectra of a reference CF-sonogel, a HNO_3 catalyzed sonogel (pH = 2.0) and the precursor reactants (TEOS, H_2O and HNO_3)

monolithic samples were obtained by the acidic route. Several catalyzed sonogels with different pH values ranging from 1.9 to 5 were obtained by this method. The lower pH samples were optically semi-transparent and faintly yellow coloured, whereas the samples having higher pH values were significantly more opaque. By contrast, the CF-sonogel samples were fully transparent through the VIS-NIR spectra, having typical pH values varying from 3 to 3.6. As shown in Fig. 2(a), the absorption spectra of a transparent and opaque acid sonogels (pH = 2 and 3.6, respectively) are compared to that of a standard CF-sample. The negligible absorption exhibited through the VIS-NIR spectra by the CF-product demonstrates the higher optical quality and purity level of our CF-samples. It can also be noticed in this figure, that the absorption increases substantially in the UV region as usual for glassy materials. In Fig. 2(b), the PL-spectra at room temperature of a CF-sample (thick solid line in black), a HNO_3 catalyzed sonogel (thin solid line in black) and the precursor materials (TEOS, HNO_3 and H_2O) of both, the CF- and acid-samples are presented. The excitation wavelength was set to $\lambda_{exc} = 350$ nm. Beside the difference on the shape of the PL-curves, it is observed that the CF-sonogel exhibits a larger PL-emission in the NUV-VIS region compared to the semi-transparent HNO_3 catalyzed sample (pH = 2.0). This fact indicates minor self-absorption effects which attenuates the PL-emission in the bulk material for the CF-sonogels. Last argument implies again, a higher transparency and purity of the CF-sonogels. The PL-bands shape exhibited by the CF-sample agrees well with the PL-spectra of typical SiO_2 glasses, which show emission in the 300–600 nm region. [1]. Additionally, two bands are clearly distinguished in the PL-emission of both, acid- and CF-sonogel samples, and are located at: 396 and 468 nm. In order to clarify the origins of these bands, the PL-emission of the precursor materials were also studied. In Fig. 2(b) the PL-emission of TEOS (thick solid line in grey), H_2O (dashed line in black) and HNO_3 (thin solid line in grey) are also presented. The PL-emissions of the precursors are considerably weaker than that observed for the two sonogel samples. The PL-emission of H_2O shows a well defined band at 396 nm and precisely matches the first band observed in both, the CF- and the catalyzed-samples. This band also coincides with one of the two bands detected in the PL-spectra of HNO_3, which is understandable since the HNO_3 solution contains $\sim$34.5% in volume of H_2O. In order to explain the band detected at 396 nm in both sonogels, the sonochemical reaction which hydrolyzes the TEOS reactant was taken into account; here, the ROH groups are bonded to the Si atoms. During condensation, oxygen bridges are formed to liberate H_2O molecules after drying. Due to the characteristic porosity of sol-gel materials, some of these H_2O molecules are trapped in the surface area of the SiO_2 network by attraction of H-bonds. The strength of this kind of bond is considerably high, so that the H_2O molecules remain within the porous structure of the SiO_2 matrix unless a thermal treatment is carried out. Last arguments can satisfactorily explain the distinctive PL-bands of H_2O detected at 396 nm in both kinds of sonogels. On the other hand, the second band detected in the PL-spectra (at 468 nm) of both sonogel samples, belonging to the SiO_2 matrix itself is probably due to the [Si–O–Si] bonds, having no apparent relation to the emission of the precursor liquid materials. The characteristic band observed in the HNO_3 PL-spectra (at 364 nm) has a noticeable influence in the PL-emission of the catalyzed sample, which shows a marked shoulder (similar slope) in the same spectral region. Finally, the PL-emission of the precursor TEOS is considerably broader and stronger than that observed for the HNO_3 and H_2O precursors, but almost two orders of magnitude weaker than that observed for the sonogels samples. The onset of its PL is similar to that of the catalyzed- and CF-samples, having a closer slope to the PL-emission detected for the CF-sample. This evidences again the purity of the CF-sonogel, which strongly follows the PL tendency of the Si-rich TEOS reactant.

The surface area generated within the porous media of the sonolyzed CF-SiO_2 matrix was estimated by the *Brunauer-*

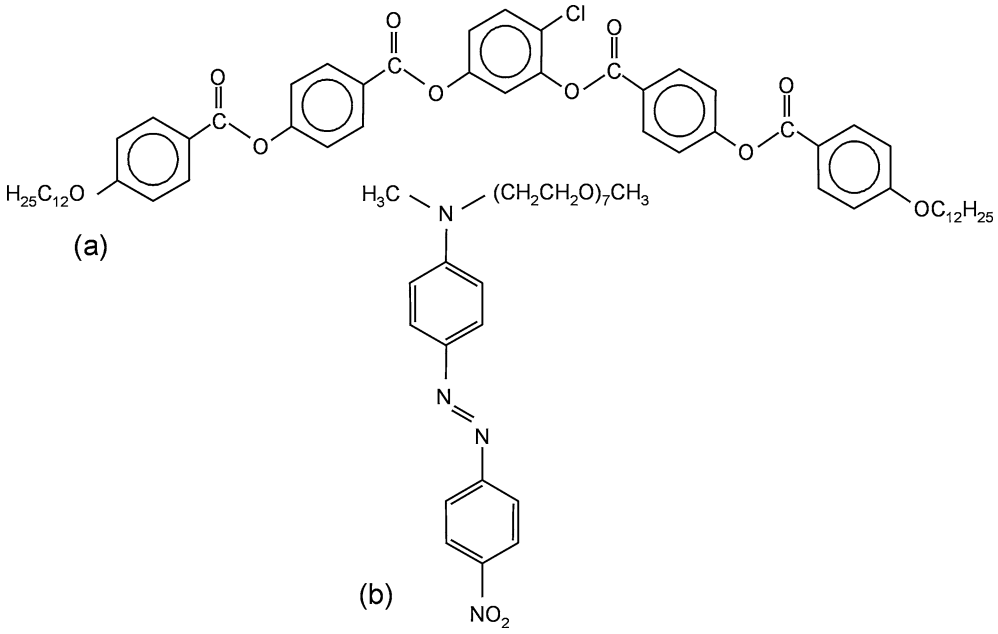

Fig. 3 Chemical structure of: (a) chlorine substituted thermotropic bent shaped mesogen and (b) RED-PEGM-7 LC azo-dye

Emmett-Teller (BET) method from 25 to 1000°C (RIG-100 equipment) [37], where 25 mg of the sonogel reference sample were analyzed. BET-studies revealed large surface areas varying from 500 to 700 $m^2\ g^{-1}$, compared to those obtained by traditional catalyst-based sol-gel methodologies. In last case, typical surface areas in the rage of 100–500 $m^2\ g^{-1}$ have been reported [1, 38]. Recently, novel methodologies have been developed for the fabrication of amorphous SiO_2 with larger surface areas, for instance the xero-gel and aerogel-route, where surface areas up to 1000 and 2000 $m^2\ g^{-1}$ have been reported, respectively. Last kind of composites are nevertheless, more expensive and difficult to synthesize [39, 40]. Beside their adequate porosity, suitable for the inclusion of dopant agents, our CF-samples showed satisfactory thermal stability from 20 to 600°C. After 600°C, the sample shows a drastic structural collapse and the average surface area drops from 650 to 2 $m^2\ g^{-1}$ as the temperature arises to 1000°C [25].

2.2 Organic dopant structures

Novel synthesized and commercial organic compounds specifically designed as active media for laser and NLO-applications were used as dopant agents to generate advanced hybrid materials by the CF-sonolysis approach. Figure 3 shows two liquid crystalline structures designed for quadratic ($\chi^{(2)}$) NLO-response. Figure 3(a) illustrates a chlorine substituted thermotropic bent shaped mesogen (4-chlororesorcinol bis[4-(4-*n*-dodecyloxybenzoyloxy)benzoate], which is soluble in tetrahydrofuran (THF) and shows new nematic and isotropic phases (homologue 12C) [27–29]. The phase transition sequence of this compound is: Crystalline, Cr: 98°C–(X-Phase: 80°C–N-Phase: 95°C)–ISO; (N) being, a nematic phase with electro-optical properties, (X) a new low temperature isotropic phase and (ISO), the liquid isotropic state. Both, the N- and X-phases exhibit monotropic behavior (phases observed on cooling only) [27–29]. Bent-shaped compounds commonly named "banana" molecules exhibit a permanent dipolar moment. This dipole is aligned along the molecular bent direction due the presence of a carboxyl- and a oxy-group (acceptor-, donator-group respectively), placed in each wing of the molecular structure. It is well known that the existence of a donor-acceptor group in organic compounds is a necessary condition for the observation of $\chi^{(2)}$-NLO effects, such as second harmonic generation (SHG). The interest to prepare hybrids with bent shaped molecules is well understood since these compounds have shown highest SHG-activity among all ever studied liquid crystalline structures [41–45].

Figure 3(b) shows the molecular structure of a novel azo-dye *N*-methyl-*N*-{4-[(*E*)-(4-nitrophenyl)diazenyl]phenyl}-*N*-(3, 6, 9, 12, 15, 18, 21-heptaoxadodeicos-1-yl)amine, named here RED-PEGM-7, which exhibits also liquid crystalline behavior and has been specifically designed for SHG applications [26]. This azo-dye can be dissolved in THF, methanol and chloroform. At room temperature, this compound forms nematic phases and can form smectic phases under visible laser irradiation, as a consequence of laser induced photo-alignment. The phase transition sequence for this compound is: Amorphous/Vitreous: (–30 to 45)°C → LC-N: (45 to 105)°C → ISO: (105 to 210)°C. RED-PEGM-7 consists basically on an amphiphilic amino-nitro substituted

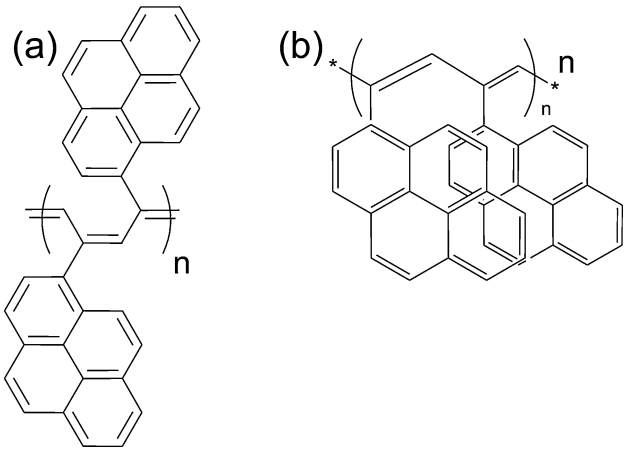

Fig. 4 Chemical structure of: (a) *cis*-poly(1-ethynylpyrene) (*cis*-PEP) and (b) *trans*-poly(1-ethynylpyrene) (*trans*-PEP)

azobenzene unit bearing an oligo(ethylene-glycol) methyl ether side chain (PEGM). The nitro and the amino substituents act as electron-withdrawing and electron-donor groups respectively. A high dipolar moment of $\mu = 8$ D has been calculated by Density Functional Theory (DFT) calculations for RED-PEGM-7, showing that this compound is very promising for NLO-applications [26, 46].

Figure 4 shows two novel conjugated poly(arylacetylenes) bearing *trans*- and *cis*- configurations. Figure 4(a) shows the *cis*-poly(1-ethynylpyrene), named *cis*-PEP [47], whereas Fig. 4(b) shows the *trans*-poly(1-ethynylpyrene), named *trans*-PEP [48]; both compounds are soluble in THF. These kind of molecular systems and homologues have been proposed for the development of optoelectronic devices such as light emitting diodes, photovoltaic cells and for NLO-applications like Third Harmonic Generation (THG), due to their conductivity and high degree of extended π-conjugation [49–52].

Four molecular structures of commercial dyes, commonly used for tunable dye laser applications in solution, were also used as dopant agents. The molecular structures and chemical details of Rhodamine 590, amino-4-methyl-2H-1-benzopyran-2-one (Coumarin 440), 2,2′-([1,1′-Biphenyl]-4,4′-diyldi-2,1-ethenediyl)-bis-benzenesulfonic acid disodium salt (Stilbene 420) and 5-amino-9-(diethylamino)-benzo[a]phenoxazin-7-ium perchlorate (Nile Blue 690), have been reported in several dye handbooks [30, 31]. Since sol-gel materials doped with dyes have been studied due to their potential in applications for tunable solid-state laser sources [12, 53, 54], the inclusion of these compounds into the developed catalyst free glasses has been also considered.

Finally, fullerene (C_{60}) spheres were also successfully used as dopant agents. C_{60} and several fullerene derivative sol-gel composites have been widely studied in recent years due to their promising technological applications such as photo-electronic, NLO and molecular sensing devices, which take advantage of their semiconducting properties.

2.3 Hybrid sample preparation

For the present application, solutions containing only 2 mg of the dopant compounds and 8 mL of solvent (THF) were prepared. In this way, a total dissolution of the dopants in the solvent was assured. The doses of the hydrolyzed-TEOS *versus* the dopant-dissolution (OH-TEOS:D-D) was prepared with a precise volumetric pipe and deposited into cylindrical teflon-containers (1 inch in diameter, 2 mL in volume) in order to obtain different doped optical glasses. It has been noted that solutions of dopants in THF are better incorporated into the CF-sonogel network, since the S_4 geometry of TEOS implies a zero dipolar moment and would not accept the inclusion of highly polar THF-based dissolutions. However, OH-TEOS becomes highly polar too and provides an optimal environment for molecules dissolved in THF (dipolar moment: $\mu = 1.6$ D). Dissolutions of molecules in toluene were fully repelled by the CF-sonogel.

Prepared hybrid materials were generated with a starting total volume of 2 mL, varying the OH-TEOS:D-D concentration ratio (in volume) as follows: 1.0:1.0, 1.2:0.8, 1.3:0.7, 1.4:0.6, 1.5:0.5, 1.6:0.4, 1.7:0.3 and 1.8:0.2 mL. Undoped sonogel samples (2:0) were also prepared for reference and calibration purposes. The samples were isolated with a plastic cover to avoid atmosphere and temperature variations and conserved for two weeks at room conditions in closed recipients with a small hole on the cap in a clean-dry-dark environment. Afterwards, the drying process of the samples was completed and the formation of bulk samples is achieved. Monolithic cylindrical samples with good optical quality, diameters varying from 8 to 12 mm and thickness varying from 0.6–1.2 mm, were obtained in most cases for very slow drying speeds (see Fig. 5).

2.4 Characterization techniques

Standard characterization techniques were applied to undoped reference sonogel samples and to several hybrid composites in order to determine their structural and optical properties. Linear optical absorption spectra were obtained in the 200–1000 nm region, using a double beam Shimadzu UV-VIS spectrophotometer, taking the air in the reference beam. Photoluminescent measurements were obtained in the same spectral range with a FluoroMax-3, Jobin-Yvon-Horiba fluorimeter and the excitation wavelength was set to $\lambda_{exc} = 250$ nm for all samples. The surface morphology of the films was studied in tapping mode by AFM (AutoProbe CP, Scanning Probe Microscope, Park Scientific Instruments). Standard DSC-measurements and the pulsed laser

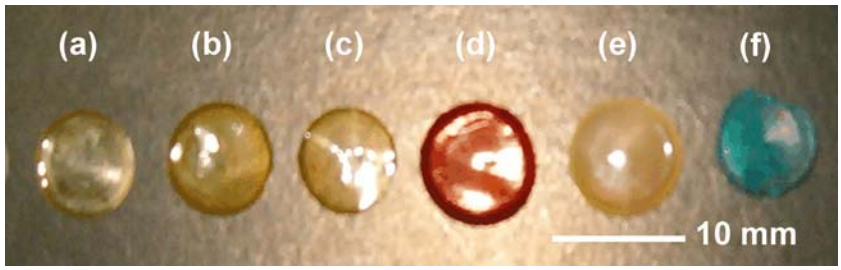

Fig. 5 Picture of different sonogel hybrid composites (geometric monoliths): (a) Reference glass, (b) Bent shaped based hybrid, (c) PEP based hybrid, (d) LC RED-PEGM-7 based hybrid, (e) Rhodamine based hybrid, and (f) Nile-Blue based hybrid

photoacoustic technique (LPAT) were also implemented in order to determine thermodynamic phase transitions of the LC-compounds embedded within the CF-sonogel environment and laser induced photo-degradation of the selected organic dyes.

3 Results and discussion

3.1 Linear optical absorption measurements

RED-PEGM-7 based hybrids, show an intense red color, heavily doped samples were only partially transparent at naked eye. Figure 6 shows the absorption spectra of different RED-PEGM-7 doped composites compared with a (2:0)-reference sample. A wide and dominant absorption band centred at 499 nm can be recognized in all samples. The red and NIR-windows present a considerable minor absorption. An enhancement of the absorption band at 500 nm with a large broadening in the blue side is also evident for heavily doped samples, which suggest the formation of H-aggregates [26]. According to Fig. 6, the absorption spectra of the lightly (1.8:0.2)-doped sample, illustrate an unsaturated transmission curve compared with those of heavily doped hybrids. This fact suggests high molecular concentration and aggregation problems for the heavy loaded composites, which are not supported by the screener action of a low mass of SiO_2 [15]. Last observations may represent a limitation for the non-linear optical response of these heavily doped composites due to intermolecular interactions caused by molecular aggregation. The evident saturation of the absorption band with increasing doping level of the samples, demonstrates a favorable inclusion of the RED-PEGM-7 compound within the SiO_2 network.

The chlorine substituted bent shaped mesogen shows strong scattering and hence an opaque yellow color within the sol-gel-phase. Figure 7 shows the absorption spectra for several bent shaped doped composites compared with that of the reference glass. Two wide absorption bands in the rage of 350–480 and 550–675 nm covering the visible region are observed for these composites. For bent-shaped based hybrids, the IR-windows present negligible absorption only. Again, the doped samples show major absorption as the doping rate increases. However, in this case, no saturation effects were observed in the absorption spectra for the same doping rates, which may be favorable for NLO- and electro-optical (EO) applications.

From the NLO point of view, deposition of spin-coated hybrid thin film layers containing last kind of LC-structures and *in-situ* poling of the trapped guest molecules will be necessary in order to achieve optimal NLO-response like

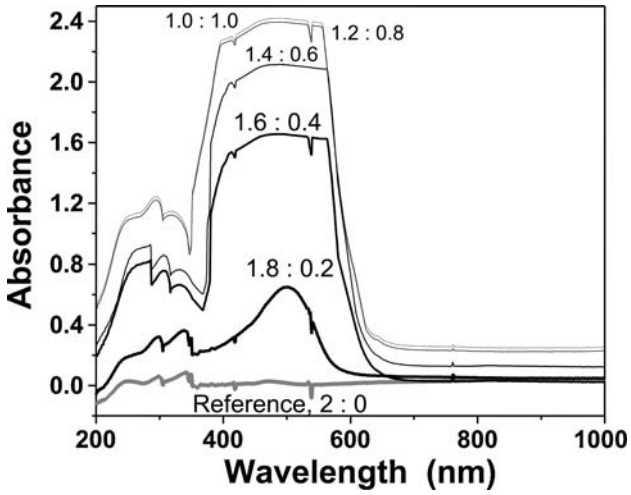

Fig. 6 Comparative absorption spectra of a reference sonogel and different RED-PEGM-7 based hybrids

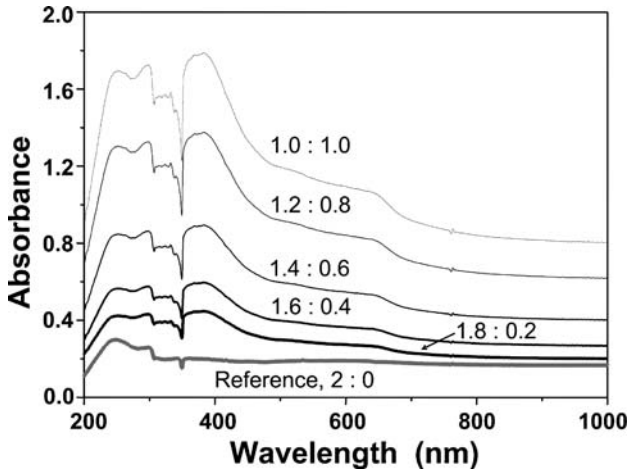

Fig. 7 Comparative absorption spectra of a reference sonogel and different Bent-Shaped based hybrids

frequency doubling (SHG), these studies are currently under way by working with the standard fundamental wave of a Nd:YAG laser system ($\lambda_\omega = 1064$ nm) and will be presented elsewhere. In the case of the chlorine substituted bent shaped mesogens, the main absorption band of the formed hybrids lay outside the SHG-line ($\lambda_{2\omega} = 532$ nm), thus large SHG signals should be expected for spin-coated *corona*-poled hybrid thin films or implementing the EFISH-technique (Electric-Field-Induced-SHG technique [55]). As mentioned before, bent shaped compounds exhibit highest quadratic NLO-response among liquid crystalline molecules [41–45]. Interestingly, preliminary results showed weak SHG-signals measured in the amorphous bulk material for these hybrid composites, where an effective nonlinear optical coefficient of about $\chi^{(2)}_{\text{eff}} = 0.08$ pm V^{-1} has been estimated according to the *Maker*-Fringes calibration technique [55]. Here an α-quartz crystal wedged in the $\chi^{(2)}_{11}$-direction ($\chi^{(2)}_{11} = 0.64$ pm V^{-1}) was implemented as standard NLO-reference. A detailed study concerning the origins of the nonlinearity for such amorphous composites will be necessary taking into account the electro-magnetic quadrupole approximation for NLO effects [56–59] or the screening effects induced by the hydrolyzed-TEOS, which reduce the dipole-dipole molecular interactions and aggregation effects [15].

On the other hand, for RED-PEGM-7 hybrid composites, the wide absorption band centred in the visible region will produce a moderated SHG-response by working with the same fundamental wave ($\lambda_\omega = 1064$ nm). Last fact was recently observed in structured RED-PEGM-8 Z-type Langmuir-Blodgett films (LB) [60], where the SHG-response was considerably absorbed although this compound exhibits a relatively high dipolar moment. For these reasons, the implementation of a tunable optical parametric oscillator (OPO-Laser system) would be required in order to provide fundamental excitation within the telecommunication wavelength range ($\lambda_\omega = 1300$–1500 nm). Under such excitation conditions, large SHG may be expected for this molecular system and could be promising for the fabrication of NLO-photonic prototypes.

Figure 8 shows the absorption spectra of some *trans*-PEP (1.3:0.7 and 1.5:0.5 samples) and *cis*-PEP (1.5:0.5 sample) based composites and are compared to that of the reference sample. Again, the absorption spectra of the hybrids increase with the dopant concentration. For comparison purposes only, a *cis*-PEP doped sample was included in the graph which clearly shows a simpler absorption spectrum. A more intense $S_2 \leftarrow S_0$ absorption band was observed for this polymer in the UV-VIS region followed by a tail due to the twisted polyacetylene backbone of the polymer. By contrast, *trans*-PEP-based materials exhibits also a $S_2 \leftarrow S_0$ absorption band at 340 nm followed by a second well defined absorption band at 600 nm due to the highly conjugated poly-

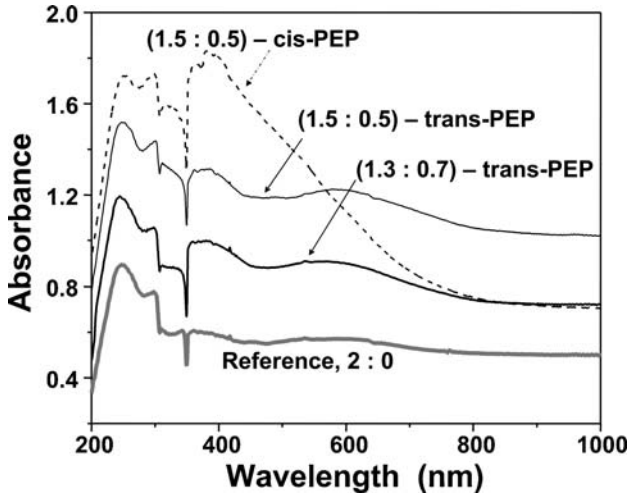

Fig. 8 Comparative absorption spectra of a reference sonogel and different *cis*-PEP and *trans*-PEP based hybrids

acetylene main chain of this polymer, for the same dopant concentration. In sol-gel, both polymers exhibit an absorption band at 340 nm due to $S_2 \leftarrow S_0$ transition of pyrene groups. This band is also observed in THF solution and appears at 350 nm (not shown here). On the other hand, the absorption spectra of *cis*-PEP in sol-gel and THF solution exhibit a second absorption band at 453 nm resulting from the formation of intramolecular pyrene-pyrene complexes in the polymer. Besides the band at 340 nm, the absorption spectrum of *trans*-PEP in sol-gel exhibits a maximum absorption wavelength at $\lambda_{\max} = 591$ nm, due to the highly conjugated polyacetylene main chain. This band is also observed in THF solution at $\lambda = 580$ nm (not shown here) [47, 48]. By contrast, *cis*-PEP shows only a tail around 570 nm, which is an indication of a lower conjugation degree in this polymer. A similar tail was also observed for *cis*-PEP in THF solution around $\lambda = 537$ nm. The fact that the lowest energy bands of *trans* and *cis*-PEP are significantly red-shifted in sol-gel compared to those observed in THF solution, reveals that in this media the polyacetylene main chain of the polymers is better aligned to planarity. This can be explained in terms of the viscosity of the environment. In solution, polymer molecules can move and display rotations along the σ bonds, whereas in sol-gel they reach their optimal conformation during the drying process. Once the sol-gel is completely dry, the rigidity of the media restrains the mobility of the molecules avoiding them to adopt other conformations. NLO-studies implementing the THG technique with *cis*-PEP, and *trans*-PEP based hybrids will be necessary in order to clarify last observations.

Fullerenes C_{60} of 99.95% purity were purchased from Aldrich and used as received. In this case and due to the low solubility of fullerenes in THF, the C_{60}-THF suspension (2 mg and 8 mL, espectiveley) was ultrasonically mixed at different ratios with the OH-TEOS. In this way, several

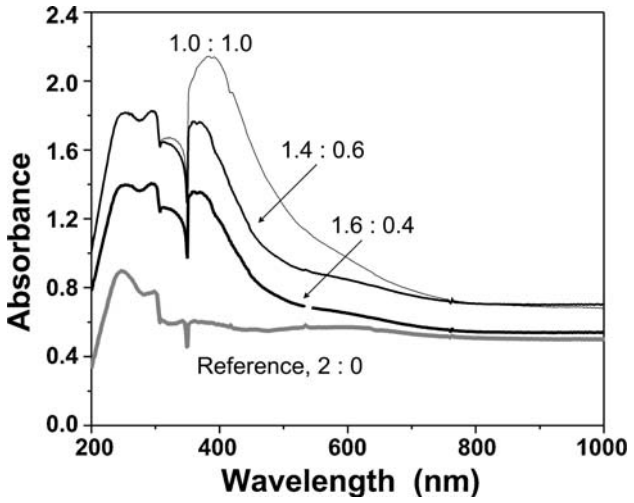

Fig. 9 Comparative absorption spectra of a reference sonogel and different C_{60} based hybrids

C_{60}-doped composites were satisfactorily obtained. As mentioned before, solutions of C_{60} in toluene were fully repelled by the OH-TEOS polarity. Absorption spectra of C_{60}-based hybrids are shown in Fig. 9. High linear absorption, typical of C_{60} and some derivatives can be observed in the violet-blue range [61, 62]. For growing doping concentration, the absorption spectra of the hybrids increase. Typical features of C_{60} in solution can be observed within the sonogel solid phase, for example, a band around 350 nm is present and corresponds to the lowest lying one photon allowed transition band. The absorption main band shows a red-shift (from 355 to around 385 nm) which could be due to intermolecular interactions between fullerene molecules in sol-gel (UV-absorption below 350 nm is mainly attributed to the sonogel matrix). The weak absorption observed in the visible region (between 400 and 750 nm) is due to the dipole-forbidden transition with the I_h structure symmetry [61–63].

3.2 Photoluminescent measurements

Classical organic dyes commonly used for tunable laser applications have been successfully used as dopant agents in the CF-sonogel samples. The resulting hybrids showed good optical and mechanical performance. PL-measurements of these composites were obtained from 200–900 nm (excitation wavelength was set at $\lambda_{exc} = 250$ nm) in order to verify the inclusion of the dye structures within the sonogel network. Figure 10 shows the PL-spectra of several doped samples. In Fig. 10(a) (continuous thin line), the PL-spectrum of a (1.5:0.5)-Rhodamine 590 based hybrid is shown. As expected, maximal emission appears in the 540–560 nm region [30, 31]. In the same figure (continuous thick line), the efficient PL of a (1.5:0.5)-Coumarin 440 based sonogel can be observed. In this case, maximal PL-emission appears in the

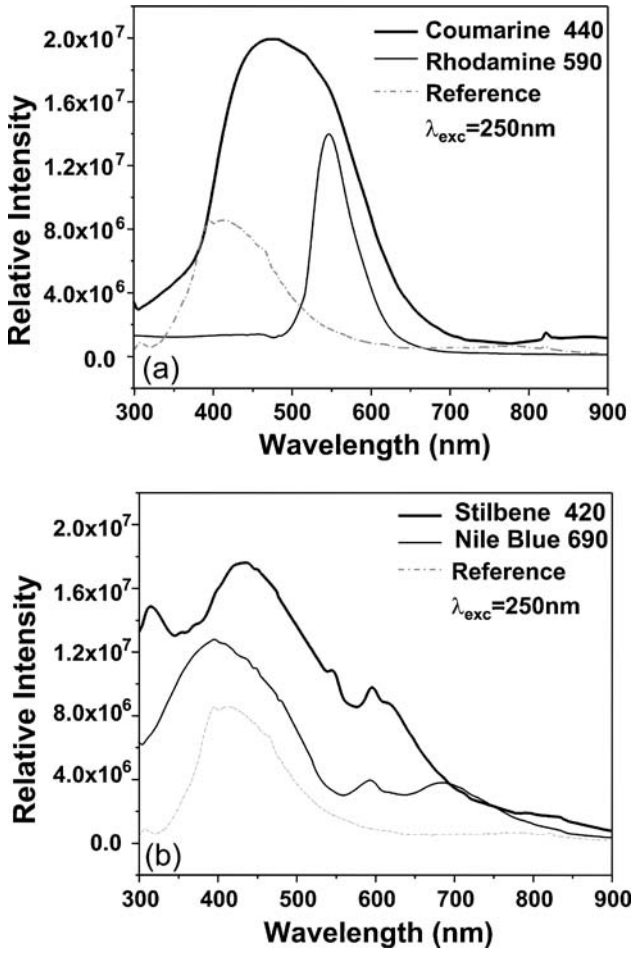

Fig. 10 Comparative PL-spectra of a reference sonogel (dashed line) and (1.5:0.5)-dye doped composites: (a) Rhodamine 590 based hybrid (solid thin line) and Coumarin 440 based sonogel (solid thick line). (b) Stilbene 420 (solid thick line) and Nile Blue 690 (solid thin line) based composites

450–510 nm spectral range in accordance with several dye laser handbooks [30, 31].

Figure 10(b) shows the fluorescence spectra of (1.5:0.5)-Stilbene 420 and (1.5:0.5)-Nile Blue 690 based composites. Three typical emission bands for the Nile Blue 690 based composite can be clearly recognized (continuous thin line): the 360–430 nm band (highest fluorescence emission), the 580–605 nm and 660–710 nm bands (moderated fluorescence emissions). These bands are commonly exploited in dye laser applications. Fluorescence spectrum of Stilbene 420 (continuous thick line) also exhibits three main emission bands, whose spectral ranges are: 307–326 nm, 420–440 nm (highest PL-emissions) and 584–619 nm (moderated PL-emission). For comparative purposes only, the PL-emission of a (2:0) reference sample is also illustrated in Fig. 10 (grey dashed line); a broad and weak emission in the 350–450 nm range can be observed: This PL-spectrum is typical of SiO_2 based glasses [1, 14].

The PL-spectrum obtained from the Nile-Blue based composites show a discrepancy with that reported in the literature data (compound in solution): the emission band centred at 685 nm in sol-gel phase is 25 nm red-shifted. All other emission bands of dye-based sonogels fits well with the literature reports, where the PL-spectra is commonly given in THF, chloroform or methanol solutions [30, 31]. In sol-gel phase, dye concentration is higher than in solution due to the shrinking process experienced by the samples with aging, which may produce aggregation problems and possible molecular interactions and bonding effects of the dopant species with the sonicated SiO_2 network. Last effects may be also responsible for the observed band shifts.

3.3 DSC and LPAT-measurements

According to DSC, and LPAT measurements, RED-PEGM-7 shows an amorphous/vitreous phase at room temperature and a liquid crystalline mesophase within the sonolyzed SiO_2 matrix. The observed thermodynamic phase transition diagrams monitored by DSC and LPAT techniques show the following sequence (see Fig. 11): Amorphous/Vitreous: (− 30 to 45)°C → LC-N: (45 to 105)°C → ISO: (105 to 210)°C. The single pulsed laser photoacoustic technique revealed higher experimental resolution compared to DSC measurements, specially for the LC-ISO transformation. In this case, an accurate response of different thermodynamic phase transitions can be unambiguously determined by the LPAT technique [64, 65]. Beyond 210°C, the hybrid starts its degradation process induced by combustion of the LC-mesogen. A shelter formed by the SiO_2 network protects the dopant agent beyond 185°C, where this molecular structure (in powder) shows thermal instability [26].

The chlorine substituted bent shaped compound show the following phase transition sequence (measured by DSC in a pure powder sample [27, 28]): Crystalline, Cr: 98°C–(X-Phase: 80°C–N-Phase: 95°C)–ISO. Figure 12 shows the thermal photoacoustic analysis of a (1.5:0.5)-bent-shaped based hybrid composite, where both, the isotropic transition (on heating) from the crystalline Cr-phase and the monotropic behavior (detected only on cooling the sample below the melting temperature) of the X- and N-mesophases can be accurately detected. A temperature phase shift of about 22°C compared with the DSC measurements performed in pure powder samples, has been observed for the monotropic-phases. In this case, the shelter formed by the SiO_2 network induced a regular phase shift over all thermodynamic phase transitions: Crystalline, Cr: 120°C–(X-Phase: 102°C–N-Phase: 117°C)–ISO.

On the other hand, tunable solid state laser applications require high optical stability of dye-based hybrids exposed to energetic laser excitation [66, 67]. For this reason, a photodegradation study of some dye-based CF-sonogel samples

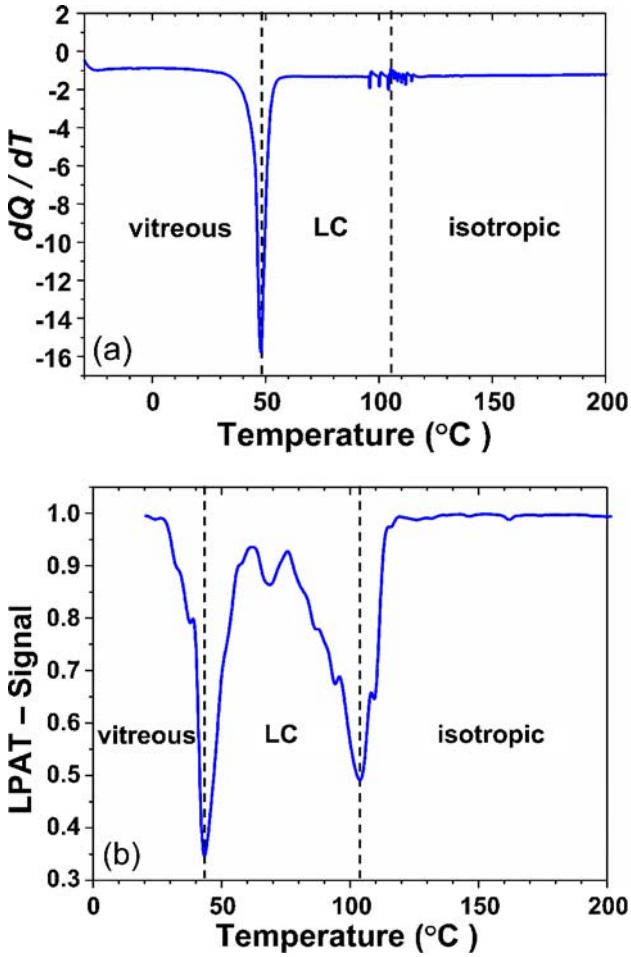

Fig. 11 Temperature phase transition diagram of a (1.5:0.5)-LC-RED-PEGM-7 based hybrid: (a) resolved by DSC (heating process, $\Delta T = 5°C\ min^{-1}$) and (b) resolved by the LPAT technique ($\Delta T = 2°C\ min^{-1}$)

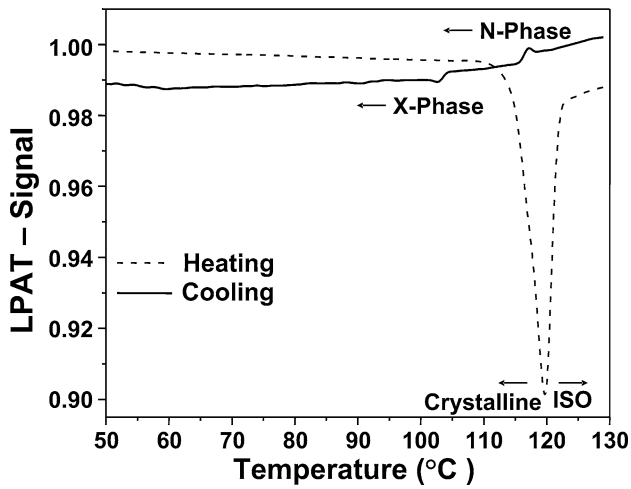

Fig. 12 Temperature phase transition diagram of a (1.5:0.5)-Bent-Shaped based hybrid resolved by the LPAT technique ($\Delta T = 2°C\ min^{-1}$)

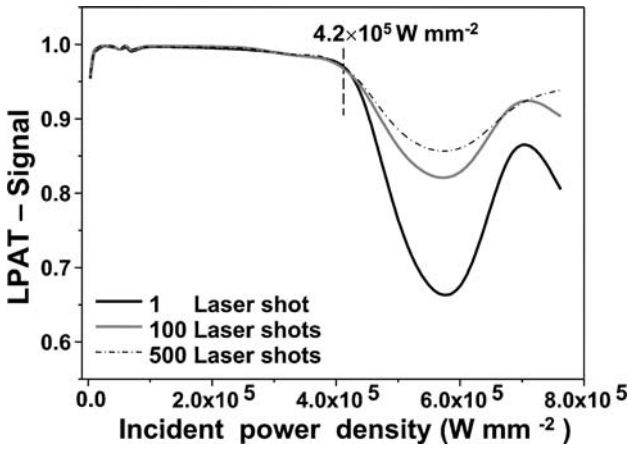

Fig. 13 Photodegradation study performed in a (1.5:0.5)-Rhodamine 590 based hybrid by the LPAT-technique with increasing pulse power density. Measurements were performed by a single laser shot (*solid black line*), 100 laser shots (*solid grey line*) and 500 laser shots (*thin dashed line*)

has been performed by the LPAT-technique. Here, the structural changes and degradation process induced by energetic pulsed laser irradiation have been monitored according to this sensitive technique [64, 65]. Since the Rhodamine 590 based hybrid exhibits large absorption in the blue-green range and Rhodamine doped silica glasses have been proven as successful laser emitters [66], therefore we performed a photo-degradation study on these samples by energetic laser irradiation obtained by the frequency doubled Nd:YAG laser system ($\lambda_{2\omega} = 532$ nm, 10 Hz, pulse width: 7 ns). Figure 13 shows the normalized photoacoustic (PA) signal of (1.5:0.5)-Rhodamine 590 based hybrids as function of the pulse power density and the number of incident pulses. The beam was focused on the sample to 2.1 mm^2 in order to achieve pulse power densities in the range of 10^5 W mm^{-2}. In Fig. 13 (solid black line) the photodegradation induced by a single pulse shot with increasing power density is monitored. High optical stability of the sample can be observed until photodegradation occurs at the laser damage threshold of $\sim 4.2 \times 10^5$ W mm^{-2}, at this power density the sample change its color from intense orange to a transparent pale-yellow, which confirms the degradation process in Rhodamine. In order to investigate the performance and optical stability of these hybrids under strong laser irradiation, the photodegradation induced by multiple laser shots with increasing power densities was also monitored (integration of the PA-signal for 100 and 500 incident laser pulses). For 100 and 500 pulse irradiation (solid grey line and dashed line, respectively), the same PA-response, and hence same optical stability was observed. Last fact clearly shows that, at least for short term applications, laser-induced photodegradation depends on the power density rather than on the irradiation time. Consequently, the CF-samples may exhibit high optical and photoemission stability as long as the pulsed laser excitation may be controlled under the observed power damage threshold value.

3.4 AFM morphology

Surface morphology and the chromophore loading mechanical stability of some sonogel hybrids were studied by high resolution AFM measurements (contact mode). For this purpose, Figs. 14 and 15 show AFM measurements of the morphology and structural dependence of the hybrids with increasing doping concentrations, where RED-PEGM-7 and *cis*-PEP bulk hybrid composites were selected. Slightly doped (1.5:0.5), and a heavily doped (1.2:0.8)-composites as well as reference samples (2:0) have been chosen in order to carry out AFM investigations. Figures 14(a) and 15(a) show

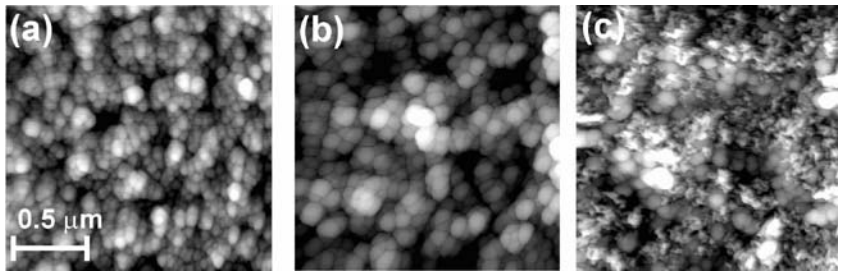

Fig. 14 AFM-scanned micrographs of different sonogel materials (same length-scale): (a) a reference sample, (b) a moderate (1.5:0.5)-RED-PEGM-7 doped sample and (c) a heavily (1.2:0.8)-RED-PEGM-7 doped sample

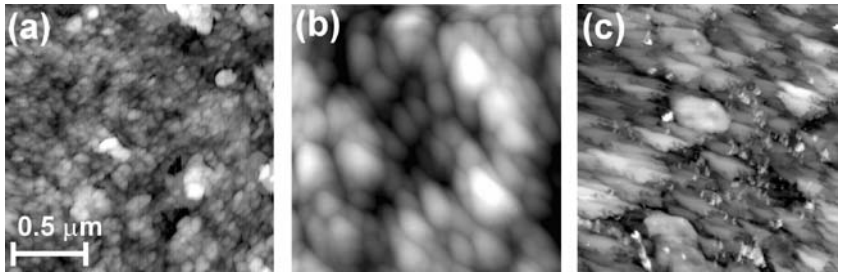

Fig. 15 AFM-scanned micrographs of different sonogel materials (same length-scale): (a) a reference sample, (b) a moderate (1.5:0.5)-cis-PEP doped sample and (c) a heavily (1.2:0.8) *cis*-PEP doped sample

the AFM-micrographs of the reference glasses obtained as the *cis*-, *trans*-PEP and RED-PEGM-7 bulk composites were prepared. These samples exhibit a stable and uniform texture with a grain size varying around 0.06–0.12 microns. Figures 14(b) and 15(b) show the AFM-micrographs of moderated doped (1.5:0.5)-hybrids (RED-PEGM-7- and *cis*-PEP bulk based hybrids, respectively). These composites also feature a stable and uniform texture, showing an enlargement of the mean grain size of up to 0.25(0.45) microns for the RED-PEGM-7(*cis*-PEP)-hybrids. The texture of these samples remains uniform in size and homogeneous without significant irregularities. Finally, Figs. 14(c) and 15(c) show the AFM-micrographs of heavily doped (1.2:0.8)-composites, these images show a clear deformation of the grain structure. The resulting irregular textures exhibit a highly disordered structure, which may be the product of molecular segregation of the dopant chromophore dissolutions within the forming SiO_2 network. All this leads to unstable structures and to the rupture of the monolithic arrangement, as has been repetitively confirmed for several hybrids after drying.

In fact, the undoped CF-reference samples always showed good mechanical quality and monolithic composition, whereas the resulting heavily doped materials featured a fractured structure after the drying time. The slightly and moderated doped samples were also mechanically stable and showed, in most cases, monolithic structures for slow drying speeds. We argue from a qualitatively analysis, that a most favorable porous size within the SiO_2 matrix should be achieved after the drying time, in which an optimal dopant concentration can be contained to produce mechanical stability. As the dopant agent is slightly added to the SiO_2 host matrix, a moderate enlargement of the constituting hybrid particles is observed. If an excessive overloading of the dopant dissolution is presented, then the solubility limit of the dopant within the gel-phase is overcome, probably a phase segregation takes place and the dopant molecules are dispersed among SiO_2 particles. As consequence, a chaotic collapse of the sample occurs during drying and the sample becomes highly unstable, the mechanical stability disappears to produce a fragile network. Best mechanical and optical properties among the studied hybrids, corresponds to the 1.6:0.4, 1.5:0.5 and 1.4:0.6 moderate doped composites. According to these studies, thin film samples are being prepared with the selected OH-TEOS:D-D concentrations in order to assure best mechanical performance for NLO-characterization.

4 Conclusions

Highly pure catalyst free SiO_2 sonogel materials were produced by the sonolysis route. The obtained materials showed large average surface areas of up to 700 $m^2\ g^{-1}$ at room temperature and mechanical stability up to 600°C. The obtained CF-sonogel glasses offered an excellent environment for the confinement of diverse organic chromophores in the colloidal state. This versatile method enabled us to prepare a large variety of hybrid samples, with the desired concentration, structure and geometry. In this work, several LC-structures, organic dyes, pyrene containing polymers and C_{60} fullerenes were successfully encapsulated within the novel CF-sonogel host matrix. The obtained samples showed monolithic structures for suitable doping and slow drying speeds. The impact of different dopant concentrations on the optical performance and mechanical stability of the studied hybrids was evaluated by absorption, PL and AFM-measurements. In most cases, the PL and linear absorption data of the doped glasses and of the corresponding solutions, overlap very well. Last facts indicate that the inclusion of dopants into the highly pure sonogel environment does not considerably affected their linear optical properties. The resulting composites exhibited good mechanical properties for an optimal OH-TEOS:D-D concentration ratio. As shown in this work, best monolithic integrity have been found for moderated doped samples (rates in volume of: 1.6:0.4, 1.5:0.5 and 1.4:0.6, total starting volume of 2 mL).

On the other hand, the LPAT technique was implemented in order to evaluate both, the molecular and optical performance of dyes and LC-compounds embedded in CF-sonogels. Different phase transitions of LC-based hybrid materials were accurately determined by this technique in order to identify interesting thermodynamic states to be optically studied. For dye-doped composites, LPAT measurements indicated high power density thresholds in the range of 4.2×10^5 W mm^{-2}, where the photo-degradation of Rhodamine-based hybrids occurs. For future investigations, Raman spectroscopy studies will be necessary in order to achieve a better understanding of the molecular interactions and bonding of the dopant species embedded within the sonicated SiO_2 network. This may help to clarify the observed PL band-shifts and the thermodynamic phase-shift transitions detected in dye and LC doped composites, respectively.

Acknowledgments Financial support from SEP-CONACYT (project: 47421) and DGAPA-PAPIIT-UNAM (projects Nr: IN-112703 and IN-112203) are gratefully acknowledged. O. G. Morales-Saavedra thanks Prof. Gerhard Pelzl (Martin-Luther University, Halle, Germany) who kindly donated the bent shaped mesogens and to the DAAD academic organization (Germany).

References

1. Brinker CJ, Scherer GW (1990) Sol-gel science: the physics and chemistry of sol-gel processing. Academic Press, San Diego
2. Fardad MA, Mishechkin OV, Fallahi M (2001) J Lightwave Technol 19(1):84
3. Zhanjia H, Liying L, Lei X, Zhiling X, Haibo L, Wencheng W, Fuming L, Mingxin Y (2001) Acta Opt Sinica 21(1):111

4. Clark A, Terpugov V, Medrano F, Cervantes M, Soto D (1999) Opt Mater 13(3):355
5. Sun XD, Wang XJ, Shan W, Song JJ, Fan M, Knobbe ET (1997) J Sol-Gel Sci Technol 9(2):169
6. Sanchez C, Leveau B (1996) Pure Appl Opt 5:689
7. Andrews MP, Najafi SI (1997) Sol-gel polymer photonic devices: critical reviews optical science and technology. SPIE-Optical Engineering Press CR68, San Diego, California
8. Reyes-Esqueda JA, Vabre L, Lacaque R, Ramz F, Forget B, Dubois A, Briat B, Boccara C, Roger G, Canva M, Lévy Y, Chaput F, Boilot JP (2003) Opt Commun 220:59
9. Pavel C, del Monte F, Worsfold DJ, Carlsson DJ, Grover ChP, Mackenzie JD (2000) Nature 408:64
10. Marino IG, Lottici PP, Bersani D, Gnappi G, Lorenzi A, Montenero A (2004) J Non-Crystall Sol 345–346:428
11. Hsiue GH, Lee RH, Jeng RJ (1999) J Poly Sci: Part A-Poly Chem 37:2503
12. Dunn B, Nishida F, Toda R, Zink LI, Allik TH, Chandra S, Hutchinson JA (1994) Advances in dye-doped sol-gel lasers: new materials for advanced solid state lasers symposium. In: Mater Res Soc, Pittsburgh, PA, USA, p 267
13. MacCraith BD, McDonagh C (2002) J Fluores 12:333
14. Sakka S (2004) Handbook of sol-gel science and technology, vol III: processing characterization and applications, Kluwer Academic Press, Boston
15. Reyes-Esqueda J, Darracq B, Garcia-Macedo J, Canva M, Blanchard-Desce M, Chaput F, Lahlil K, Boilot JP, Brun A, Levy Y (2001) Opt Commun 198:207
16. Choi DH, Lim SJ, Jahng WS, Kim N (1996) Thin Solid Films 287:220
17. Hosoya Y, Ohsugi S, Muto S, Kurokawa Y (1996) Thin Solid Films 283:221
18. Liying L, Lei X, Zhanjia H, Zhiling X, Jie C, Wencheng W, Fuming L (1999) Phys Lett A 262:206
19. Kajzar F, Swalen DJ (1996) Organic thin films for waveguiding nonlinear optics. Gordon and Breach Publishers, San Diego
20. Rauch S, Selbmann Ch, Bault P, Sawade H, Heppke G, Morales-Saavedra O, Huang MYM, Jkli A (2004) Phys Rev E 69: 021707
21. Selvarajan A (2001) IEEE J Quantum Elect 37:1117
22. Priebe G, Kunze K, Kentischer F, Schulz R, Morales O, Macdonald R, Eichler HJ (2000) In: 45th SPIE annual meeting vol 3143. SPIE-Optical Engineering Press, San Diego, California, p128
23. Wilkes GL, Orler B, Huang HH (1985) Poly Prep 26:300
24. Morikawa A, Iyoku Y, Kakimoto M, Imai YJ (1992) Mater Chem 26:79
25. Flores-Flores JO, Saniger JM (2006) Catalyst-free SiO_2 sonogels. J Sol-Gel Sci Technol 39:235
26. Rivera E, Belletête M, Natansohn A, Durocher G (2003) Can J Chem 81:1076
27. Pelzl G, Eremin A, Diele S, Kresse H, Weissflog W (2002) J Mater Chem 12:2591
28. Weissflog W, Sokolowski S, Dehne H, Das B, Grande S, Schroder MW, Eremin A, Diele S, Pelzl G, Kresse H (2004) Liq Cryst 31(7):923
29. Eremin A, Diele S, Pelzl G, Weissflog W (2003) Phys Rev E 67:020, 702
30. Eastman-Kodak (1990) Cataloge No 54, Laboratory Chemicals, International Edition, USA
31. Lambdachrome Laser Dyes (1986) Lambda-physik cataloge, 1st edition, Göttingen, Germany
32. Suslick KS (1990) Science 247:1373
33. de la Rosa-Fox N, Esquivias L, Zarzycki J (1987) Diffusion and Defect Data 53–54:363
34. Suslick KS (1986) Adv Organ Chem 25:73
35. Noltingk BE, Neppiras EA (1950) Proc Phys Soc B 63:674
36. Esquivias L, de la Rosa-Fox N (2003) J Sol-Gel Sci Technol 26:651
37. Greggand SJ, Sing KSW (1982) Adsorption, surface area and porosity, Academic Press, London
38. Sherer GW (1999) Cement and Concret Res 29:1149–1157
39. Smirnova I (2002) Synthesis of silica aerogels and their application as a drug delivery system. Dissertation, TU-Berlin, Germany
40. Saraidarov T, Reisfeld R, Pietraszkiewicz M (2000) Chem Phys Lett 330:515
41. Macdonald R, Kentischer F, Warnick P, Heppke G (1998) Phys Rev Lett 81:4408
42. Morales-Saavedra OG, Bulat M, Rauch S, Heppke G (2004) Mol Cryst Liq Cryst 413:607
43. Ortega J, Pereda N, Folcia CL, Extebarria J, Ros MB (2000) Phys Rev E 63:011702
44. Morales Saavedra OG (2003) Spatially resolved second harmonic microscopy in novel bent shaped liquid crystalline mesogens and applications to organic QPM-waveguiding structures. Dissertation, W&T Verlag, ISBN: 3-89820-477-4, TU-Berlin, Germany
45. Ortega J, Gallastegui JA, Folcia CL, Etxebarra J, Gimeno N, Ros MB (2004) Liq Crys 31:579
46. Morales-Saavedra OG, Castañeda R, Villagran-Muniz M, Flores-Flores JO, Bañuelos JG, Saniger JM, Rivera E (2006) Mol Cryst Liq Cryst 449:161
47. Rivera E, Wang R, Zhu XX, Zargarian D, Giasson R (2003) J Mole Catalysis A: Chem 204–205:325
48. Rivera E, Belletête M, Zhu XX, Durocher G, Giasson R (2002) Polymer 43:5059
49. Friend RH, Gymer RW, Holmes AB, Burroughes JH, Marks RN, Taliani C, Bradley DDC, Dos Santos DA, Bredas JL, Logdlund M, Salanek WR (1999) Nature 397:121
50. Heeger AJ (2001) Angew Chem Int Ed Engl 40:2591
51. Bernius MT, Inbasekaran M, O'Brien J, Wu WS (2000) Adv Mater 12:1737
52. Morales-Saavedra OG, Rivera E (2006) Linear and non linear optical properties of trans and cis-poly(1-ethynylpyrene) based sonogel hybrid materials, Polymer 47:5330, DOI: 101016/jpolymer200605042
53. Reisfeld (2002) J Fluorescence 12(314):317
54. Schultheiss S, Yariv E, Reisfeld R, Breur HD (2002) Photochem Photobiol Dvi 1(5):320
55. Prasad PN, Williams DJ (1991) Introduction to nonlinear optical effects in molecules and polymers. Wiley Inter Sciences, New York, p 117
56. Shtykov NM, Barnik MI, Beresnev LA, Blinov LM (1985) Mol Cryst Liq Cryst 124:379
57. Zhong-Can OY, Yu-Zhang X (1985) Phys Rev A 32:189
58. Arakelyan SM (1981) Mol Cryst Liq Cryst 71:137
59. Shtykov NM, Blinov LM, Dorozhkin AM, Barnik MI (1982) Pis'ma Zh Eksp Teor Fiz 35:142
60. Rivera E, Carreón-Castro MP, Rodriguez L, Cedillo G, Rodríguez L, Fomine S, Morales-Saavedra OG (2006) Dyes, Pigments, DOI: 101016/jdyepig200602023
61. Kano S, Kohno M, Sakiyama K, Sasaki S, Aya N, Shimura H (2003) Chem Phys Lett 378:474
62. Wang HL, Grigorova M, Maniloff ES, McBranch DW, Mattes BR (1997) Shynthetic Mater 84:253
63. Dou K, Du JY, Knobbe ET (1999) J Luminesc 83–84:241
64. Pineda-Flores JL, Castañeda-Guzmn R, Villagrn-Muniz M, Huanosta TA (2001) Apply Phys Lett 79(8):1166
65. Marchi MC, Castañeda-Guzmn R, Pérez-Pacheco A, Bilmes SA, Villagrn-Muñiz M (2004) Int J Thermophys 25(2):491
66. Altman JC, Stone RE, Dunn B, Nishida F (1991) IEEE Photonics Tech Lett 3:189
67. Dunn B, Nishida F, Toda R, Zink JI, Allic TH, Chandra S, Hutchinson JA (1994) Mat Res Soc Symp Proc 329:267